HHS Public Access

Author manuscript

Neuroscience. Author manuscript; available in PMC 2018 July 31.

Published in final edited form as:

Neuroscience. 2018 February 10; 371: 254–267. doi:10.1016/j.neuroscience.2017.11.025.

Neuroanatomical distribution of DEK protein in corticolimbic circuits associated with learning and memory in adult male and female mice

Valentina Ghisays[1], **Elizabeth T. Nguyen**[2], **Joshua Streicher**[3], **Nicholas A. Pease**[4], **Maureen Fitzgerald**[4], **Christina M. Estrada**[1], **Ana Franco-Villanueva**[4], **Lisa Privette Vinnedge**[3], and **Matia B. Solomon**[2,4]

[1]Experimental Psychology Graduate Program, Univ. of Cincinnati, Cincinnati, OH

[2]Neuroscience Graduate Program, Univ. of Cincinnati, Cincinnati, OH

[3]Division of Oncology, Cancer and Blood Diseases Institute, Cincinnati Children's Hospital Medical Center, Cincinnati, OH

[4]Department of Psychiatry and Behavioral Neuroscience Univ. of Cincinnati, Cincinnati, OH

Abstract

DEK, a chromatin-remodeling gene expressed in most human tissues, is known for its role in cancer biology and autoimmune diseases. DEK depletion *in vitro* reduces cellular proliferation, induces DNA damage subsequently leading to apoptosis, and down-regulates canonical Wnt/β-catenin signaling, a molecular pathway essential for learning and memory. Despite a recognized role in cancer (non-neuronal) cells, DEK expression and function is not well characterized in the central nervous system. We conducted a gene ontology analysis (ToppGene), using a cancer database to identify genes associated with DEK deficiency, which pinpointed several genes associated with cognitive-related diseases (i.e., Alzheimer's disease, presenile dementia). Based on this information, we examined DEK expression in corticolimbic structures associated with learning and memory in adult male and female mice using immunohistochemistry. DEK was expressed throughout the brain in both sexes, including the medial prefrontal cortex (prelimbic, infralimbic and dorsal peduncular). DEK was also abundant in all amygdalar subdivisions (basolateral, central and medial) and in the hippocampus including the CA1, CA2, CA3, dentate gyrus (DG), ventral subiculum and entorhinal cortex. Of note, compared to males, females had significantly higher DEK immunoreactivity in the CA1, indicating a sex difference in this region. DEK was co-expressed with neuronal and microglial markers in the CA1 and DG, whereas only a small percentage of DEK cells were in apposition to astrocytes in these areas. Given the reported inverse cellular and molecular profiles (e.g., cell survival, Wnt pathway) between cancer and Alzheimer's disease, these findings suggest a potentially important role of DEK in cognition.

Corresponding Author: Matia B. Solomon PhD, University of Cincinnati, Department of Psychiatry and Behavioral Neuroscience, Metabolic Diseases Institute Bldg A Room 131, 2170 East Galbraith Rd./ML-0506, Reading, OH 45237-1625.

Keywords

cognition; hippocampus; oncogene; learning and memory; Wnt pathway; sex differences; Alzheimer's disease

Introduction

Aberrant expression or localization of the DEK DNA-binding protein has been associated with several diseases, including acute myeloid leukemia (Logan et al 2015, Von Lindern et al 1992), various types of solid tumors (Piao et al 2014, Privette Vinnedge et al 2015, Wang et al 2014), and as an auto-antigen in numerous auto-immune diseases, most notably juvenile idiopathic arthritis (Mor-Vaknin et al 2011, Sierakowska et al 1993, Szer et al 1994). DEK (human 6p22.3) is a unique protein, with no known homologs, that preferentially binds supercoiled and cruciform DNA *in vitro*. DEK is primarily expressed in proliferating cells, largely due to transcriptional regulation of *DEK* by the E2F family of transcription factors and steroid hormone receptors (Carro et al 2006, Privette Vinnedge et al 2012). Therefore, it is frequently over-expressed in solid tumors, especially melanoma (Khodadoust et al 2009, Riveiro-Falkenbach et al 2017), breast cancer (Privette Vinnedge et al 2012, Privette Vinnedge et al 2011), and human papilloma virus (HPV)-induced cancers including cervical cancer (Liu et al 2012, Wise-Draper et al 2005, Wu et al 2008) and head and neck squamous cell carcinomas (Adams et al 2015a, Adams et al 2015b). DEK can be localized intracellularly and extracellularly. However, its tissue-specific expression and intracellular function(s) in non-diseased tissue remain poorly defined.

Due to its unique nucleic acid-binding properties, DEK has been implicated in several cellular processes, including DNA replication, DNA repair, chromatin remodeling, transcription activation and repression, and mRNA splicing (Riveiro-Falkenbach & Soengas 2010, Wise-Draper et al 2009a). The characterization of DEK as an oncogene is attributed to its intracellular properties. For example, DEK localized within the nucleus is associated with DNA repair, and its overexpression is anti-apoptotic, promotes cellular proliferation, and prevents differentiation (Kappes et al 2008, Privette Vinnedge et al 2015, Wise-Draper et al 2006, Wise-Draper et al 2009b). In contrast, DEK deficiency induces DNA damage, likely due to insufficient DNA repair, as well as cellular senescence, and apoptosis (Kavanaugh et al 2011, Kim et al 2009). DEK is not only expressed intracellularly but also can be found extracellularly in biofluids, such as synovial fluid. DEK is secreted by macrophages under proinflammatory conditions where it can serve as a chemotactic molecule for neutrophils, CD8+ T lymphocytes, and natural killer (NK) cells. Furthermore, *in vitro* models using macrophages and HeLa cells demonstrated that extracellular DEK can be taken in by neighboring epithelial cells through a heparan sulfate-dependent process, and then translocate back into the nucleus to perform its chromatin modifying functions (Saha et al 2013). High DEK levels in the extracellular space is associated with autoimmune disorders including juvenile rheumatoid arthritis, due to the synthesis of auto-antibodies against DEK (Mor-Vaknin et al 2011, Sierakowska et al 1993).

The cellular proliferative effects of DEK in the periphery are mediated in part via the transcription of Wnt ligands and subsequent activation of the canonical Wnt/β-catenin signaling pathway (Privette Vinnedge et al 2015, Privette Vinnedge et al 2012). Accordingly, DEK deficiency in cancer cells and mouse embryonic fibroblasts down-regulates the canonical Wnt pathway, a critical molecular pathway for learning and memory. In the brain, Wnt proteins are essential for proper maintenance and function of the hippocampal formation (Fortress et al 2013). Specifically, the canonical Wnt/β-catenin pathway plays a key role in synaptic plasticity and the formation of memories within the hippocampus and the amygdala (Fortress & Frick 2016, Fortress et al 2013, Riise et al 2015). Although *DEK* mRNA expression has been reported in the adult human brain, with greater expression in malignant versus healthy brain tissue (Kroes et al 2000), the neuroanatomical distribution of DEK protein in the murine adult brain has not been characterized. Given the association between DEK in the periphery with the Wnt signaling pathway, and because DEK deficiency gives rise to many of the cellular and molecular anomalies associated with cognitive dysfunction (DNA damage, apoptosis, cellular senescence), the goal of this study was to characterize DEK protein expression in brain regions associated with various forms of learning and memory (medial prefrontal cortex, hippocampus, and amygdala).

DEK is an estrogen receptor responsive target gene (Privette Vinnedge et al 2012). As such, we examined DEK expression in both adult male and female brains. Based on the aforementioned findings, we hypothesized that DEK protein expression would be abundant in corticolimbic structures regulating learning and memory and that DEK expression would be higher in females relative to males. We report that DEK is ubiquitously expressed throughout adult male and female murine brain and that DEK is co-expressed with neurons, astrocytes, and microglia in the dentate gyrus. Indeed, we also note a sex difference in the brain, with a higher number of DEK-positive cells in the CA1 region of the hippocampus of adult female mice.

Experimental Procedures

RNA Sequencing

Previously reported RNA-Sequencing data was acquired from the NCBI Gene Expression Omnibus Series accession number GSE70462. Briefly, the human head and neck squamous cell carcinoma (HNSCC) cell line UM-SCC-1 was transduced with lentiviral pLKO.1 vector with either nontargeting control shRNA (NTsh) or DEK shRNA (DEK832; Sigma-Aldrich Mission shRNA library). Following selection in puromycin, RNA was purified and analyzed on an Illumina HiSeq2500 for single-end sequencing with 50 base pair reads (Adams et al 2015a).

Animals

Dek knockout mice—In order to determine antibody specificity, adult female Dek $^{-/-}$ knockout (KO) mice (n=6) and wild-type (WT) littermate controls (n=5) obtained from Cincinnati Children's Medical Hospital were used. Dek KO mice were generated by using a targeting-construct containing 8.6 kb of genomic DNA with the *IRES-LacZ-Neo* selectable

marker inserted into NsiI site in exon 6 (Broxmeyer et al 2012, Wise-Draper et al 2009a) and were backcrossed into a C57BL/6 background.

DEK expression in corticolimbic circuits—Male (n=8) and female (n=8) 12-week old C57BL/6 mice from Jackson Laboratories (Bar Harbor, ME) were used to determine DEK expression in corticolimbic circuits associated with learning and memory.

DEK co-expression with neurons, astrocytes and microglia—A separate cohort of animals male (n=8) and female (n=8) 12-week old C57BL/6 mice from Jackson Laboratories (Bar Harbor, ME) were used to determine if DEK was expressed in neurons, astrocytes, and microglia in the hippocampus. Because DEK is an estrogen receptor (ER) α target gene (Privette Vinnedge et al 2012), the estrous phase of cycling mice was determined at the end of the study using previously published methods (Becker et al., 2005).

All animals used in this study were placed on a reversed 12-h light/dark cycle (lights on at 1000 h) with *ad libitum* access to food (Purina rodent chow) and water. All procedures were approved by the University of Cincinnati IACUC and Cincinnati Children's Hospital IACUC.

Tissue collection—Mice were deeply anesthetized with an overdose of sodium pentobarbital and transcardially perfused with 0.9% saline followed by 4% paraformaldehyde in 0.1M sodium phosphate-buffered (PBS; pH 7.6). Brains were carefully removed from the skull and post-fixed in 4% PFA in 0.1M PBS (pH 7.6) for 24 h at 4°C. Brains were then incubated in 30% sucrose in 0.1M PBS and stored at 4°C. Brains were sectioned in a one in six series on a freezing microtome (Leica; 35 μm thickness) and stored in cryoprotectant solution (0.1M PBS, 1% w/r polyvinylpyrrolidone (PVP) 30% v/v ethylene glycol, 30% w/v sucrose) at −20°C until processing (Solomon et al 2015).

Immunohistochemistry—For DEK antibody specificity and characterization in brain, coronal brain sections were incubated in 1% H_2O_2 for 10 min, rinsed with 0.1M PBS (pH 7.6), and blocked with 4% Normal Goat Serum (NGS)/0.4% Triton-X in 0.1M PBS for 1 h. Sections were incubated overnight at room temperature with the primary anti-DEK antibody (1:1000; Proteintech cat. #16448-1-AP) diluted in blocking solution. The next day brain sections were rinsed in 0.1M PBS and then incubated for 1 h in goat-anti rabbit biotinylated secondary (1:500; Vector Laboratories, Burlingame, CA). Sections were washed again in 0.1M PBS and then incubated in the Avidin Biotin Complex (ABC) elite kit (1:800; Vector Laboratories, Burlingame, CA) for 1 h followed by 0.1M PBS washes. Finally, sections were incubated in a solution of 3,3-diaminobenzidine tetrahydrochloride (DAB) tablets (10 mg/tablet; Sigma-Aldrich, St. Louis, MO), and mounted in a 3% gelatin/0.1M PBS solution onto ultrastick slides (Gold Seal, Portsmouth, NH). Sections were dehydrated with a graded alcohol series of 50%, 70%, 95%, and 100% (2x) ethanol followed by xylene (2x) and coverslipped with DPX mounting medium (Sigma-Aldrich, St. Louis, MO) (Solomon et al 2015).

Dual Immunofluorescence—Dual fluorescent immunolabeling was performed on coronal brain sections labeled with primary antibodies raised against DEK and neuronal

nuclei (NeuN), DEK and astrocytes (GFAP), or DEK and microglia (IBA-1). Sections were incubated in 1% H_2O_2 for 10 min, rinsed with 0.1M PBS, and blocked with 0.05 mol/L Tris-HCL buffer containing 0.1% Tween, 0.015 mol/L sodium azide, and stabilizing proteins to reduce background (Dako North America, Inc., cat. #S3022, Carpinteria, CA) for 1hr prior to incubation with rabbit polyclonal anti-DEK (1:1000; Proteintech cat. #16448-1-AP) and mouse monoclonal anti-GFAP (1:200; Millipore, Billerica, MA) or mouse monoclonal anti-NeuN (1:1600; Millipore, Billerica, MA) diluted in blocking solution (Dako diluent) overnight at room temperature. The following day sections were rinsed 5 times in 0.1M PBS followed by incubation in Cy3 donkey anti-mouse IgG (1:500; Jackson ImmunoResearch, West Grove, PA) and Cy5 goat anti-rabbit IgG (1:500; Thermo Fisher Scientific, Rockford, IL) for 1 h at room temperature. Sections were then rinsed in 0.1M PBS and mounted in a 3% gelatin/0.1M PBS solution onto Ultrastick slides (Gold Seal, Portsmouth, NH). Sections were coverslipped with polyvinyl alcohol anti-fading medium with DABCO (Sigma-Aldrich, St. Louis, MO). For DEK and microglia (IBA-1), sections were also incubated in 1% H_2O_2 for 10 min, rinsed with 0.1M PBS, and blocked with Dako diluent for 1 h prior to incubation with rabbit polyclonal anti-DEK overnight at room temperature. On day 2, sections were rinsed 5 times in 0.1M PBS followed by incubation in Cy5 goat anti-rabbit IgG (1:500) for 1 h at room temperature. Sections were rinsed again in 0.1M PBS, blocked for 2 h in Dako diluent, and incubated overnight in IBA-1 (1:7000; Wako Chemicals, Cambridge, MA) at room temperature. On day three, sections were rinsed in 0.1M PBS followed by incubation in Alexa Fluor Plus 488 goat anti-rabbit IgG (1:500; Thermo Fisher Scientific, Rockford, IL) for 45 min h at room temperature. Sections were then rinsed in 0.1M PBS and mounted in a 3% gelatin/0.1M PBS solution onto Ultrastick slides (Gold Seal, Portsmouth, NH). Sections were coverslipped with polyvinyl alcohol anti-fading medium with DABCO (Sigma-Aldrich, St. Louis, MO).

Immunohistochemical Image Analyses—Targeted brain regions were selected according to the nomenclature and nuclear boundaries of Paxinos and Franklin mouse brain atlas 2nd edition. DEK expression was assessed in the following regions: prelimbic cortex (PrL), infralimbic cortex (IL), dorsal peduncular cortex (DP), medial amygdala (MeA), central amygdala (CeA), basolateral amygdala (BLA), dorsal hippocampal formation (CA1, CA2, CA3, dentate gyrus), ventral subiculum (VS), and entorhinal cortex (EC) (Fig. 1). Images were captured at 5x, 10x, or 20x magnification with Carl Zeiss Imager Z.1 (Carl Zeiss Microimaging, Thornwood, New York), exported into ImageJ software (National Institutes of Health, Bethesda, Maryland) and counted using the thresholding technique. Bilateral cell counts were quantified by two observers who were blind to group identify (i.e., sex or genotype). The interrater reliability for cell counts was 91.2%. For each brain region of interest, unilateral counts from two to four bilateral sections were averaged together to determine region-specific DEK expression for that animal. The final DEK-positive cell counts was reported as the number of immunoreactive cells per unit area and expressed as positive nuclei per unit area (mm^2) for each group.

Image Analysis for Co-Expression—After processing, dual stained sections were analyzed using the Nikon confocal laser microscope system C2si+ (Nikon Instruments Inc., Melville, NY), equipped with epi-fluorescence attachment and filters. Images were captured

and analyzed with NIS-Elements C imaging and AR analysis software. Excitation of FITC labelling for the detection of Alexa Fluor Plus in microglia was done using the 488 nm diode laser. For excitation of Cy5 (DEK) and Cy3 (NeuN or GFAP) fluorophores, a 640 nm and 543 nm diode laser was used, respectively. 5 × 5 large-stitched images taken with the PlanApo λ 40x objective were collected from 8–9 individual frames separated by a stepwise depth of 1.0–1.2 μm in the z-axis per animal. The Landweber deconvolution method to denoise and enhance contrast based on wavelet deconvolution was used on resulting 3D image z stacks uniformly (Vonesch & Unser 2008). Using large-stitched image multichannel thresholding in NIS-Elements AR analysis software, positive immunoreactive cells were thresholded for each individual channel (e.g., Cy5, Cy3, or Alexa488) within brain regions of interest. The merged image was then overlaid with the intersection of both single-channel thresholds to define co-expressions (e.g., Alexa488 HAVING Cy5). DEK positive staining was visualized using 640 nm wavelength but designated a pseudo green color for illustrative purposes to enhance contrast with NeuN and GFAP in red, and designated a pseudo red color for greater contrast with IBA-1 in green.

Statistical analyses

Statistical analyses were performed using SPSS (version 20) statistical software. An independent sample t-test or Mann Whitney U test was used to compare the final number of DEK positive cells for each brain region between males and females. Data sets were checked for normality using the Shapiro-Wilk normality test and homogeneity of variance with the Levene's test. When normal distribution and equal variances were met, the means between groups were compared using an independent sample-t-test. The non-parametric Mann-Whitney U test was used for data that were not normally distributed. Outliers were identified and subsequently removed from statistically analyses using the Grubb's test (Barnett & Lewis, 1994). In additional to significance testing, Cohen's d was calculated to express effect sizes. The effect size represents the magnitude of the difference between groups. Cohen's d of .2=small, .5=medium, and .8=large effect sizes, respectively. For t-tests, data are presented as means and standard error of the means and for Mann Whitney U analyses; the data are presented as median with the range. Statistical significance was set at $p<0.05$

Results

DEK deficiency is associated with cognitive-related diseases

Genes up-regulated by more than 2-fold were used for gene ontology analysis using ToppGene to identify DEK loss associated diseases (Chen et al 2009). Consistent with previous findings, inflammatory-related (black) and cancer-related (blue) genes were identified (Table 1). Notably, these analyses also revealed a number of genes associated with various cognitive related diseases (red). Of the cognitive related diseases, 73 genes were associated with Alzheimer's disease, presenile dementia (44 genes), dementia (35 genes), senile plaques (25 genes), plaque amyloid (28 genes), age-related cognitive decline (5 genes), and severe dementia (5 genes).

DEK distribution in corticolimbic circuits associated with learning and memory

Brain sections from Dek KO mice (n=6) and WT controls (n=5) were processed for DEK immunohistochemistry to determine antibody specificity.. DEK immunoreactivity is robustly expressed in the medial prefrontal cortex in WT controls (Fig. 2A), but absent in the Dek KO mice (Fig. 2B). Figure 2C illustrates DEK immunoreactivity in the dorsal hippocampus in WT mice; however, there is no DEK immunolabeling in the dorsal hippocampus in Dek KO mice (Fig. 2D). Figures 2E and 2F capture DEK immunoreactivity in amgydalar subdivisions in WT and Dek KO mice, respectively. DEK immunolabeling is prominently expressed in the entorhinal cortex and ventral subiculum in WT mice (Fig. 2G), but noticeably absent in the Dek KO mice (Fig. 2H). The robust difference in DEK expression between the two genotypes indicates antibody specificity using this genetic control method. Thus, the specificity of this antibody is validated by the lack of DEK immunolabeling in Dek KO mice.

DEK positive cells were ubiquitously expressed throughout the brain in both males (n=8) and females (n=8), albeit to varying degrees. In the present study, we quantified DEK protein expression in predetermined corticolimbic regions of interest including the medial prefrontal cortex, amygdala (basolateral, central, and medial), dorsal hippocampus (CA1, CA2, CA3, and dentate gyrus), ventral subiculum, and entorhinal cortex.

Prefrontal Cortex

DEK was robustly expressed in female and male prelimbic and infralimbic cortices (Figs. 3A–3D) and the dorsal peduncular nucleus (Figs. 3E–3F). There was no sex difference in DEK expression in the prelimbic [t(14)=1.97, p=0.06, d=.98, Fig. 3G], infralimbic [t(14)=1.03, p>0.05, d=.52, Fig. 3H], or the dorsal peduncular nucleus [t(14)=1.78, p>0.05, d=.89, Fig. 3I].

Amygdala

DEK was abundantly expressed in the medial and basolateral (Figs. 4A–4F) amygdala nuclei in males and females. Prior to medial amygdala analyses, one male and one female were removed as they were deemed outliers, which resulted in a final group size for males (n=7) and females (n=7). A Mann-Whitney test indicated no sex difference in DEK expression in the medial amygdala [$U_{7,7}$ = 24.0, p >0.05; d=.20, Fig. 6G]. There was no sex difference in DEK expression in the basolateral amygdala [t(14)=.95, p>0.05, d=.48], as shown in Fig. 4H. DEK was also abundantly expressed in the central amygdala (Figs. 5A–5D). Although there was a slight trend, there was no sex difference in DEK expression in the central amygdala [t(14)=2.3, p=0.06, d=.89]; as illustrated in Fig. 5E.

Hippocampus

One female was removed from the CA2, entorhinal cortex, and ventral subiculum analyses; therefore the final group size for each of these brain regions was male (n=8) and female (n=7). DEK was expressed in all regions of the hippocampal formation including the CA1, CA2, and CA3 (stratum oriens (SO), stratum pyramidale (SP), stratum radiatum (SR)), all layers in the dentate gyrus (DG) (molecular (ML), polymorph (PL), granular (GCL) and

subgranular (SGZ) zones), and ventral subiculum. DEK was moderately expressed in the CA1 and CA2 subdivisions in females and males (Figs.6A–6F).

A Mann-Whitney test indicated that the number of DEK-positive cells in the CA1 was greater for females than for males [$U_{8,8}$ = 13.0, p = .04, d=1.39; Fig. 6G]. However, there was no significant sex difference in DEK expression in the CA2 [t(13)=1.59, d=.83, p>0.05]; refer to Fig 6H. A representative immunohistochemical image of DEK expression in the CA3 and DG in females and males is illustrated in Figures 7A–7F. There was no sex difference in DEK expression in the CA3 [t(14)= 0.16, p>0.05, d=0.1, Fig. 7G] or in the DG [t(14)=0.08, p>0.05, d=0.04, Fig. 7H]. Figures 8A–8F illustrate DEK immunoreactivity in the entorhinal cortex and ventral subiculum in the female and male brains. There was no sex difference in DEK expression in the ventral subiculum [t(13)=0.98, p>0.05, d=.67, Fig. 8G] or entorhinal cortex [t(13)=1.26, p>0.05, d=.51, Fig 8H].

Hippocampal DEK co-expression with neuronal, astrocytic and microglial markers

The goal of this experiment was to assess the percentages of DEK positive cells in the CA1 and DG subregions of the dorsal hippocampus that express the markers for neurons, astrocytes, or microglia with dual label immunohistochemistry. Given that DEK is highly expressed in proliferating cells, its expression in major cell types in the dentate gyrus, as a substantial site for neurogenesis throughout the lifespan was assessed (Zhao et al., 2008). In addition, because there was a sex difference in DEK expression in the CA1, DEK expression in major cell types in this sub-region was assessed as well. Approximately 25% and 15% of DEK cells were co-expressed with the neuronal marker NeuN in the CA1 in females and males, respectively. There was no sex difference in the percentage of DEK-NeuN co-expression in the CA1 [t(14)=1.45, p>0.05, d=.72]. Consistent with the CA1, there was no sex difference in the percentage of DEK expression in neurons [t(14) = 1.44, p>0.05, d=.72] in the DG. However, there was a greater percentage of co-expression with DEK and NeuN in this area in both males (69%) and females (89%). Approximately 10% of DEK expressing cells in the CA1 were in apposition to astrocytes in both males and females; as such, there is no sex difference in the percentage of co-expression [t(14)=.0.63, d=0.05, p>0.05]. Only 2% of DEK expressing cells in this region co-express with GFAP in females and males; hence, there is no sex difference in the percentage of this co-expression [t(14)= 0.09, d=.32, p>0.05]. There is no sex difference in the percentage of DEK and IBA-1 co-expression [t(14)=0.19, d=0.52, p>0.05] in the CA1, with both males and females having about 20% co-expression in this hippocampal subdivision. Similar to the other markers, there is no sex difference in the percentage of co-expression with DEK and IBA-1 [t(14)=1.04, d=0.08, p>0.05]. Both females (59%) and males (64%) had a large percentage of DEK co-expression with IBA-1 in the DG (data not shown).

Discussion

Gene ontology analyses of human head and neck cancer (HNSCC) cells identified Alzheimer’s and other cognitive-related diseases as candidate DEK-loss associated diseases, suggesting DEK may be critical for learning and memory. Based on the information gathered from the ToppGene gene ontology analyses, we examined DEK protein expression

in cognitive relevant brain regions in the adult murine brain, including the prefrontal cortex, amygdala, and hippocampus. Furthermore, because DEK is an ERα responsive target gene (Privette Vinnedge et al 2012), we examined its expression in adult male and female murine brain.

Of the targeted regions, the CA1 region of the dorsal hippocampus was the only brain region with significantly higher DEK immunolabeling in females relative to males. Whether this sex difference in DEK expression is biologically significant or due to organizational or activational effects of gonadal hormones remains to be determined as we utilized randomly cycling females for the immunohistochemical analyses. Expression of various markers for synaptic or morphological plasticity within the CA1 region is sensitive to gonadal hormones (Parducz et al 2006, Shors et al 2004). Although we did not control for the estrous cycle, per se, knowing the stage of the estrous cycle at the time of termination in the second experiment allowed us to briefly assess any variability in DEK expression that may be due to fluctuations in gonadal hormones. Upon close inspection of the data, the variability in final cell counts for DEK, as well as other markers (i.e., neurons, astrocytes and microglia) across brain regions was not limited to sex. In some instances, males had similar, lower, or more variability in cell counts relative to females suggesting that any potential variability between the two is not solely due to the activational effects of gonadal hormones. However, future studies should delve further into a potential role for gonadal hormones to regulate DEK expression and function in the brain in both males and females.

DEK expression was most prominent in the dentate gyrus. This is noteworthy because the dentate gyrus is one of two sites in the adult central nervous system (CNS) where neurogenesis occurs (Drew et al 2013). *In vitro* studies indicate that Wnt/β-catenin signaling is necessary and sufficient for adult hippocampal neurogenesis (Lie et al 2005). Cultured hippocampal progenitors express Wnt ligands and receptors, that when co-cultured with astrocytes, respond to astrocyte-derived Wnts, inducing differentiation of these progenitors into neurons (Lie et al 2005, Wexler et al 2009). In the periphery, the cellular proliferative effects of DEK are in part mediated via the canonical Wnt/β-catenin signaling pathway (Privette Vinnedge et al 2015). Given the critical role of hippocampal Wnt signaling in learning and memory, future studies will explore the cellular and behavioral consequences of the interaction between DEK and Wnt/β-catenin signaling in this region. Since cellular proliferation in the brain is restricted to areas such as the hippocampus, we wanted to determine which cell types within this region express DEK. Here, we report that DEK is prominently expressed in neurons and microglia in the dentate gyrus and moderately (20%) expressed in these cell types in the CA1. Although, we did not find a high percentage of co-expression between DEK and GFAP in these targeted areas, this finding does not imply that the relatively low co-expression between these two markers is not meaningful or that there will not be higher percentages of co-expression in other hippocampal subdivisions (i.e., hilus) or other brain regions. At present, the functional role for DEK within these cellular types in the CNS has not been established. These findings do however suggest that DEK may interact with either of these cell types in the hippocampus to modulate cellular, physiological, or behavioral processes (cognition). Here, we describe DEK co-expression with neuronal, astrocytic, and microglial markers in the brain of healthy young adult female and male mice. Because of the prominent role of DEK in cancer and autoimmune diseases, it

is likely that its expression alone, co-expression with the aforementioned markers, and perhaps overall function in the CNS may differ under other circumstances (e.g., aging, obesity, Alzheimer's disease). Examining how this protein functions in a healthy and diseased brain is critical towards understanding its function in the CNS.

DEK is expressed in most human tissues (Sanden et al 2014) and plays a role in both transcriptional activation and gene transrepression (Campillos et al 2003, Sammons et al 2006). However, we are still in the infancy stage of understanding its defined role in gene regulation. To date, the only factors known to directly modulate DEK transcription are E2F-1, YY-1, NF-Y and estrogen receptor (ER)α (Carro et al 2006, Privette Vinnedge et al 2012, Sitwala et al 2002). Consistent with DEK overexpression in tumors or proliferating cells, these factors are also expressed at higher rates in cancer (Privette Vinnedge et al 2011) and are associated with either cellular or behavioral indices of learning and memory (Aubry et al 2015, Bean et al 2014, Gurtner et al 2010, Rossner et al 2006, Ting et al 2014, Vierk et al 2014). While DEK is known for its role in cancer and autoimmune diseases (Matrka et al 2015, Mor-Vaknin et al 2011, Pease et al 2015), its function in the CNS has not been described. DEK mRNA expression has been reported in mouse (http://www.brain-map.org/) and human brains (Kroes et al 2000), but to our knowledge, no studies have investigated protein expression nor neuroanatomical distribution in distinct brain regions. In the human adult brain, DEK mRNA expression is more heavily expressed in malignant brain tumors relative to normal controls (Kroes et al 2000), consistent with the reported increase of DEK expression in various cancers including breast (Privette Vinnedge et al 2015), bladder (Datta et al 2011) and gastric (Piao et al 2014). DEK mRNA is also expressed throughout the brain in adolescent (PND56) male mice, which is consistent with our observations in adult mice. Herein, we report that DEK protein is abundantly expressed in healthy adult murine brains in regions associated with learning, memory, and neurogenesis.

To our knowledge, we are the first to characterize and quantify DEK protein expression in the adult male and female murine brain in corticolimbic structures related to various forms of learning and memory including the medial prefrontal cortex, amygdala, and hippocampus. The assertion that DEK may be a player in cognition is plausible, given our ToppGene analyses revealing many genes related to cognitive dysfunction due to DEK deficiency and subsequent detection of its expression in brain regions associated with learning and memory. Although this is the first study to suggest an association between the DEK oncogene and cognitive dysfunction, the link between cancer and Alzheimer's disease has been proposed. In short, epidemiological data suggests an inverse transcriptional profile between cancer and neurodegenerative diseases, like Alzheimer's (Driver et al 2015, Lanni et al 2012, McShea et al 2007, Pavlides et al 2010, Raina et al 2000, Zhu et al 2000). For example, cancer is associated with increased cellular proliferation (Stopper et al 2003), decreased apoptosis (Gerl & Vaux 2005), up-regulation of the canonical Wnt-pathway (Segditsas & Tomlinson 2006, Zhan et al 2017), while Alzheimer's disease is associated with DNA damage (Coppede & Migliore 2009, Lovell & Markesbery 2007), decreased neurogenesis (Demars et al 2010), apoptosis (Smale et al 1995), and down-regulation of the canonical Wnt-pathway (Riise et al 2015). DEK deficiency *in vitro* or in the periphery induces cellular and molecular anomalies commonly observed in neurodegenerative diseases including DNA damage, cellular senescence, decreased cellular proliferation, and down-

regulation of the canonical Wnt-pathway (Kavanaugh et al 2011, Matrka et al 2015, Saha et al 2013, Tabbert et al 2006). In this same vein, DEK expression facilitates DNA repair, is anti-apoptotic (through p53 dependent and independent mechanisms), promotes cellular proliferation, and prevents differentiation (Wise-Draper et al 2006, Wise-Draper et al 2009b). Taken together, this suggests that intracellular DEK may have a protective effect against some of the cellular and molecular signatures often observed in neurodegenerative diseases.

Conclusions and Limitations

Given the existing data regarding the role of DEK in the periphery on cellular and molecular pathways associated with learning and memory, we hypothesized that DEK may function as a novel player in cognition. Indeed, our findings illustrate prominent DEK expression in the cognition-related brain regions including the medial prefrontal cortex, amygdala, and hippocampus. Because DEK was prominently expressed in major cell types (i.e., neurons, microglia) in the dentate gyrus and CA1, this postulate is not out of the realm of possibility. We acknowledge that the data presented herein are correlative in nature and that simply describing the neuroanatomical distribution of DEK in these targeted brain regions does not indicate a functional significance in learning and memory. In addition, we also recognize that the noted cellular and molecular phenotypes in the periphery that occur with DEK depletion or overexpression may not translate to the CNS. Further, we note that the identified cognition-related phenotype that emerged from our ToppGene analysis was due to DEK deficiency in diseased cells (i.e., HNSCC). As such, this same phenotype may not occur in healthy cells. However, based on the findings from the present study, we propose that future studies should explore the necessity and sufficiency of DEK in learning and memory.

Acknowledgments

Funding for this work was in part provided by Eunice Kennedy Shriver National Institute of Child Health & Human Development of the National Institutes of Health under Award Number K12HD051953 to Joel Tsevat (PI), LMPV (K12 Scholar), and MBS (K12 Scholar), and from the Local Initiative for Excellence (L.I.F.E.) Foundation to MBS and LMPV.

Abbreviations

BLA	basolateral amygdaloid complex
CA	cornu ammonis
CeA	central amygdaloid complex
CNS	central nervous system
DG	dentate gyrus
DP	dorsal peduncular cortex
ENT	entorhinal cortex

GCL	granule cell layer
IL	infralimbic cortex
MeA	medial amygdaloid complex
ML	molecular layer
mPFC	medial prefrontal cortex
PL	polymorphic layer
PrL	prelimbic cortex
SGZ	subgranular zone
SL	stratum lacunosum moleculare
SO	stratum oriens
SP	stratum pyramidale
SR	stratum radiatum
VS	ventral subiculum
shRNA	short-hairpin RNA
HNSCC	human head and neck squamous cell carcinoma

References

Adams AK, Bolanos LC, Dexheimer PJ, Karns RA, Aronow BJ, et al. IRAK1 is a novel DEK transcriptional target and is essential for head and neck cancer cell survival. Oncotarget. 2015a; 6:43395–407. [PubMed: 26527316]

Adams AK, Hallenbeck GE, Casper KA, Patil YJ, Wilson KM, et al. DEK promotes HPV-positive and -negative head and neck cancer cell proliferation. Oncogene. 2015b; 34:868–77. [PubMed: 24608431]

Aubry S, Shin W, Crary JF, Lefort R, Qureshi YH, et al. Assembly and interrogation of Alzheimer's disease genetic networks reveal novel regulators of progression. PloS one. 2015; 10:1–25.

BarnettV, , LewisT. Outliers in statistical data3. New York: John Wiley, Sons; 1994

Bean LA, Ianov L, Foster TC. Estrogen receptors, the hippocampus, and memory. Neuroscientist. 2014; 20:534–45. [PubMed: 24510074]

Broxmeyer HE, Kappes F, Mor-Vaknin N, Legendre M, Kinzfogl J, et al. DEK regulates hematopoietic stem engraftment and progenitor cell proliferation. Stem Cells Dev. 2012; 21:1449–54. [PubMed: 21943234]

Campillos M, Garcia MA, Valdivieso F, Vazquez J. Transcriptional activation by AP-2alpha is modulated by the oncogene DEK. Nucleic acids research. 2003; 31:1571–5. [PubMed: 12595566]

Carro MS, Spiga FM, Quarto M, Di Ninni V, Volorio S, et al. DEK Expression is controlled by E2F and deregulated in diverse tumor types. Cell Cycle. 2006; 5:1202–7. [PubMed: 16721057]

Chen J, Bardes EE, Aronow BJ, Jegga AG. ToppGene Suite for gene list enrichment analysis and candidate gene prioritization. Nucleic acids research. 2009; 37:W305–11. [PubMed: 19465376]

Coppede F, Migliore L. DNA damage and repair in Alzheimer's disease. Current Alzheimer research. 2009; 6:36–47. [PubMed: 19199873]

Datta A, Adelson ME, Mogilevkin Y, Mordechai E, Sidi AA, Trama JP. Oncoprotein DEK as a tissue and urinary biomarker for bladder cancer. BMC Cancer. 2011; 11:234. [PubMed: 21663673]

Demars M, Hu YS, Gadadhar A, Lazarov O. Impaired neurogenesis is an early event in the etiology of familial Alzheimer's disease in transgenic mice. Journal of neuroscience research. 2010; 88:2103–17. [PubMed: 20209626]

Drew LJ, Fusi S, Hen R. Adult neurogenesis in the mammalian hippocampus: why the dentate gyrus? Learning & memory. 2013; 20:710–29. [PubMed: 24255101]

Driver JA, Zhou XZ, Lu KP. Pin1 dysregulation helps to explain the inverse association between cancer and Alzheimer's disease. Biochimica et biophysica acta. 2015; 1850:2069–76. [PubMed: 25583562]

Fortress AM, Frick KM. Hippocampal Wnt Signaling: Memory Regulation and Hormone Interactions. The Neuroscientist: a review journal bringing neurobiology, neurology and psychiatry. 2016; 22:278–94.

Fortress AM, Schram SL, Tuscher JJ, Frick KM. Canonical Wnt signaling is necessary for object recognition memory consolidation. The Journal of neuroscience: the official journal of the Society for Neuroscience. 2013; 33:12619–26. [PubMed: 23904598]

Gerl R, Vaux DL. Apoptosis in the development and treatment of cancer. Carcinogenesis. 2005; 26:263–70. [PubMed: 15375012]

Gurtner A, Fuschi P, Martelli F, Manni I, Artuso S, et al. Transcription factor NF-Y induces apoptosis in cells expressing wild-type p53 through E2F1 upregulation and p53 activation. Cancer Res. 2010; 70:9711–20. [PubMed: 20952509]

Kappes F, Fahrer J, Khodadoust MS, Tabbert A, Strasser C, et al. DEK is a poly(ADP-ribose) acceptor in apoptosis and mediates resistance to genotoxic stress. Molecular and cellular biology. 2008; 28:3245–57. [PubMed: 18332104]

Kavanaugh GM, Wise-Draper TM, Morreale RJ, Morrison MA, Gole B, et al. The human DEK oncogene regulates DNA damage response signaling and repair. Nucleic acids research. 2011; 39:7465–76. [PubMed: 21653549]

Khodadoust MS, Verhaegen M, Kappes F, Riveiro-Falkenbach E, Cigudosa JC, et al. Melanoma proliferation and chemoresistance controlled by the DEK oncogene. Cancer research. 2009; 69:6405–13. [PubMed: 19679545]

Kim DW, Chae JI, Kim JY, Pak JH, Koo DB, et al. Proteomic analysis of apoptosis related proteins regulated by proto-oncogene protein DEK. J Cell Biochem. 2009; 106:1048–59. [PubMed: 19229864]

Kroes RA, Jastrow A, McLone MG, Yamamoto H, Colley P, et al. The identification of novel therapeutic targets for the treatment of malignant brain tumors. Cancer Lett. 2000; 156:191–8. [PubMed: 10880769]

Lanni C, Racchi M, Memo M, Govoni S, Uberti D. p53 at the crossroads between cancer and neurodegeneration. Free radical biology & medicine. 2012; 52:1727–33. [PubMed: 22387179]

Lie DC, Colamarino SA, Song HJ, Desire L, Mira H, et al. Wnt signalling regulates adult hippocampal neurogenesis. Nature. 2005; 437:1370–5. [PubMed: 16251967]

Liu K, Feng T, Liu J, Zhong M, Zhang S. Silencing of the DEK gene induces apoptosis and senescence in CaSki cervical carcinoma cells via the up-regulation of NF-kappaB p65. Bioscience reports. 2012; 32:323–32. [PubMed: 22390170]

Logan GE, Mor-Vaknin N, Braunschweig T, Jost E, Schmidt PV, et al. DEK oncogene expression during normal hematopoiesis and in Acute Myeloid Leukemia (AML). Blood cells, molecules & diseases. 2015; 54:123–31.

Lovell MA, Markesbery WR. Oxidative DNA damage in mild cognitive impairment and late-stage Alzheimer's disease. Nucleic acids research. 2007; 35:7497–504. [PubMed: 17947327]

Matrka MC, Hennigan RF, Kappes F, DeLay ML, Lambert PF, et al. DEK over-expression promotes mitotic defects and micronucleus formation. Cell Cycle. 2015; 14:3939–53. [PubMed: 25945971]

McShea A, Lee HG, Petersen RB, Casadesus G, Vincent I, et al. Neuronal cell cycle re-entry mediates Alzheimer disease-type changes. Biochimica et biophysica acta. 2007; 1772:467–72. [PubMed: 17095196]

Mor-Vaknin N, Kappes F, Dick AE, Legendre M, Damoc C, et al. DEK in the synovium of patients with juvenile idiopathic arthritis: characterization of DEK antibodies and posttranslational modification of the DEK autoantigen. Arthritis Rheum. 2011; 63:556–67. [PubMed: 21280010]

Parducz A, Hajszan T, Maclusky NJ, Hoyk Z, Csakvari E, et al. Synaptic remodeling induced by gonadal hormones: neuronal plasticity as a mediator of neuroendocrine and behavioral responses to steroids. Neuroscience. 2006; 138:977–85. [PubMed: 16310961]

Pavlides S, Tsirigos A, Vera I, Flomenberg N, Frank PG, et al. Transcriptional evidence for the "Reverse Warburg Effect" in human breast cancer tumor stroma and metastasis: similarities with oxidative stress, inflammation, Alzheimer's disease, and "Neuron-Glia Metabolic Coupling". Aging. 2010; 2:185–99. [PubMed: 20442453]

Pease NA, Wise-Draper T, Privette Vinnedge L. Dissecting the Potential Interplay of DEK Functions in Inflammation and Cancer. J Oncol. 2015; 2015:106517. [PubMed: 26425120]

Piao J, Shang Y, Liu S, Piao Y, Cui X, et al. High expression of DEK predicts poor prognosis of gastric adenocarcinoma. Diagn Pathol. 2014; 9:67. [PubMed: 24650035]

Privette Vinnedge LM, Benight NM, Wagh PK, Pease NA, Nashu MA, et al. The DEK oncogene promotes cellular proliferation through paracrine Wnt signaling in Ron receptor-positive breast cancers. Oncogene. 2015; 34:2325–36. [PubMed: 24954505]

Privette Vinnedge LM, Ho SM, Wikenheiser-Brokamp KA, Wells SI. The DEK oncogene is a target of steroid hormone receptor signaling in breast cancer. PloS one. 2012; 7:e46985. [PubMed: 23071688]

Privette Vinnedge LM, McClaine R, Wagh PK, Wikenheiser-Brokamp KA, Waltz SE, Wells SI. The human DEK oncogene stimulates beta-catenin signaling, invasion and mammosphere formation in breast cancer. Oncogene. 2011; 30:2741–52. [PubMed: 21317931]

Raina AK, Zhu X, Rottkamp CA, Monteiro M, Takeda A, Smith MA. Cyclin' toward dementia: cell cycle abnormalities and abortive oncogenesis in Alzheimer disease. Journal of neuroscience research. 2000; 61:128–33. [PubMed: 10878584]

Riise J, Plath N, Pakkenberg B, Parachikova A. Aberrant Wnt signaling pathway in medial temporal lobe structures of Alzheimer's disease. Journal of neural transmission. 2015; 122:1303–18. [PubMed: 25680440]

Riveiro-Falkenbach E, Ruano Y, Garcia-Martin RM, Lora D, Cifdaloz M, et al. DEK oncogene is overexpressed during melanoma progression. Pigm Cell Melanoma R. 2017; 30:194–202.

Riveiro-Falkenbach E, Soengas MS. Control of tumorigenesis and chemoresistance by the DEK oncogene. Clin Cancer Res. 2010; 16:2932–8. [PubMed: 20501624]

Rossner S, Sastre M, Bourne K, Lichtenthaler SF. Transcriptional and translational regulation of BACE1 expression--implications for Alzheimer's disease. Progress in neurobiology. 2006; 79:95–111. [PubMed: 16904810]

Saha AK, Kappes F, Mundade A, Deutzmann A, Rosmarin DM, et al. Intercellular trafficking of the nuclear oncoprotein DEK. Proceedings of the National Academy of Sciences of the United States of America. 2013; 110:6847–52. [PubMed: 23569252]

Sammons M, Wan SS, Vogel NL, Mientjes EJ, Grosveld G, Ashburner BP. Negative regulation of the RelA/p65 transactivation function by the product of the DEK proto-oncogene. The Journal of biological chemistry. 2006; 281:26802–12. [PubMed: 16829531]

Sanden C, Jarvstrat L, Lennartsson A, Brattas PL, Nilsson B, Gullberg U. The DEK oncoprotein binds to highly and ubiquitously expressed genes with a dual role in their transcriptional regulation. Mol Cancer. 2014; 13:215. [PubMed: 25216995]

Segditsas S, Tomlinson I. Colorectal cancer and genetic alterations in the Wnt pathway. Oncogene. 2006; 25:7531–7. [PubMed: 17143297]

Shors TJ, Falduto J, Leuner B. The opposite effects of stress on dendritic spines in male vs. female rats are NMDA receptor-dependent. The European journal of neuroscience. 2004; 19:145–50. [PubMed: 14750972]

Sierakowska H, Williams KR, Szer IS, Szer W. The putative oncoprotein DEK, part of a chimera protein associated with acute myeloid leukaemia, is an autoantigen in juvenile rheumatoid arthritis. Clin Exp Immunol. 1993; 94:435–9. [PubMed: 8252804]

Sitwala KV, Adams K, Markovitz DM. YY1 and NF-Y binding sites regulate the transcriptional activity of the dek and dek-can promoter. Oncogene. 2002; 21:8862–70. [PubMed: 12483538]

Smale G, Nichols NR, Brady DR, Finch CE, Horton WE Jr. Evidence for apoptotic cell death in Alzheimer's disease. Experimental neurology. 1995; 133:225–30. [PubMed: 7544290]

Solomon MB, Loftspring M, de Kloet AD, Ghosal S, Jankord R, et al. Neuroendocrine Function After Hypothalamic Depletion of Glucocorticoid Receptors in Male and Female Mice. Endocrinology. 2015; 156:2843–53. [PubMed: 26046806]

Stopper H, Schmitt E, Gregor C, Mueller SO, Fischer WH. Increased cell proliferation is associated with genomic instability: elevated micronuclei frequencies in estradiol-treated human ovarian cancer cells. Mutagenesis. 2003; 18:243–7. [PubMed: 12714689]

Szer IS, Sierakowska H, Szer W. A novel autoantibody to the putative oncoprotein DEK in pauciarticular onset juvenile rheumatoid arthritis. The Journal of rheumatology. 1994; 21:2136–42. [PubMed: 7869324]

Tabbert A, Kappes F, Knippers R, Kellermann J, Lottspeich F, Ferrando-May E. Hypophosphorylation of the architectural chromatin protein DEK in death-receptor-induced apoptosis revealed by the isotope coded protein label proteomic platform. Proteomics. 2006; 6:5758–72. [PubMed: 17001602]

Ting JH, Marks DR, Schleidt SS, Wu JN, Zyskind JW, et al. Targeted gene mutation of E2F1 evokes age-dependent synaptic disruption and behavioral deficits. J Neurochem. 2014; 129:850–63. [PubMed: 24460902]

Vierk R, Brandt N, Rune GM. Hippocampal estradiol synthesis and its significance for hippocampal synaptic stability in male and female animals. Neuroscience. 2014; 274:24–32. [PubMed: 24846612]

Von Lindern M, Fornerod M, Soekarman N, Van Baal S, Jaegle M, et al. Translocation t(6;9) in acute non-lymphocytic leukaemia results in the formation of a DEK-CAN fusion gene. Bail Cl Hae. 1992; 5:857–79.

Vonesch C, Unser M. A fast thresholded landweber algorithm for wavelet-regularized multidimensional deconvolution. IEEE transactions on image processing: a publication of the IEEE Signal Processing Society. 2008; 17:539–49. [PubMed: 18390362]

Wang X, Lin L, Ren X, Lin Z, Li Z, et al. High expression of oncoprotein DEK predicts poor prognosis of small cell lung cancer. International journal of clinical and experimental pathology. 2014; 7:5016–23. [PubMed: 25197373]

Wexler EM, Paucer A, Kornblum HI, Palmer TD, Geschwind DH. Endogenous Wnt signaling maintains neural progenitor cell potency. Stem Cells. 2009; 27:1130–41. [PubMed: 19418460]

Wise-Draper TM, Allen HV, Jones EE, Habash KB, Matsuo H, Wells SI. Apoptosis inhibition by the human DEK oncoprotein involves interference with p53 functions. Molecular and cellular biology. 2006; 26:7506–19. [PubMed: 16894028]

Wise-Draper TM, Allen HV, Thobe MN, Jones EE, Habash KB, et al. The human DEK proto-oncogene is a senescence inhibitor and an upregulated target of high-risk human papillomavirus E7. Journal of virology. 2005; 79:14309–17. [PubMed: 16254365]

Wise-Draper TM, Mintz-Cole RA, Morris TA, Simpson DS, Wikenheiser-Brokamp KA, et al. Overexpression of the cellular DEK protein promotes epithelial transformation in vitro and in vivo. Cancer research. 2009a; 69:1792–9. [PubMed: 19223548]

Wise-Draper TM, Morreale RJ, Morris TA, Mintz-Cole RA, Hoskins EE, et al. DEK proto-oncogene expression interferes with the normal epithelial differentiation program. The American journal of pathology. 2009b; 174:71–81. [PubMed: 19036808]

Wu Q, Li Z, Lin H, Han L, Liu S, Lin Z. DEK overexpression in uterine cervical cancers. Pathol Int. 2008; 58:378–82. [PubMed: 18477217]

Zhan T, Rindtorff N, Boutros M. Wnt signaling in cancer. Oncogene. 2017; 36:1461–73. [PubMed: 27617575]

Zhu X, Raina AK, Boux H, Simmons ZL, Takeda A, Smith MA. Activation of oncogenic pathways in degenerating neurons in Alzheimer disease. International journal of developmental neuroscience: the official journal of the International Society for Developmental Neuroscience. 2000; 18:433–7. [PubMed: 10817927]

Highlights

- Gene ontology analyses reveal for the first time that DEK deficiency is associated with cognitive-related diseases
- DEK is robustly expressed throughout adult male and female murine brain
- DEK immunoreactivity is greater in the CA1 region of hippocampus in adult females compared with adult males
- DEK is co-expressed with neurons, astrocytes, and microglia in the hippocampus

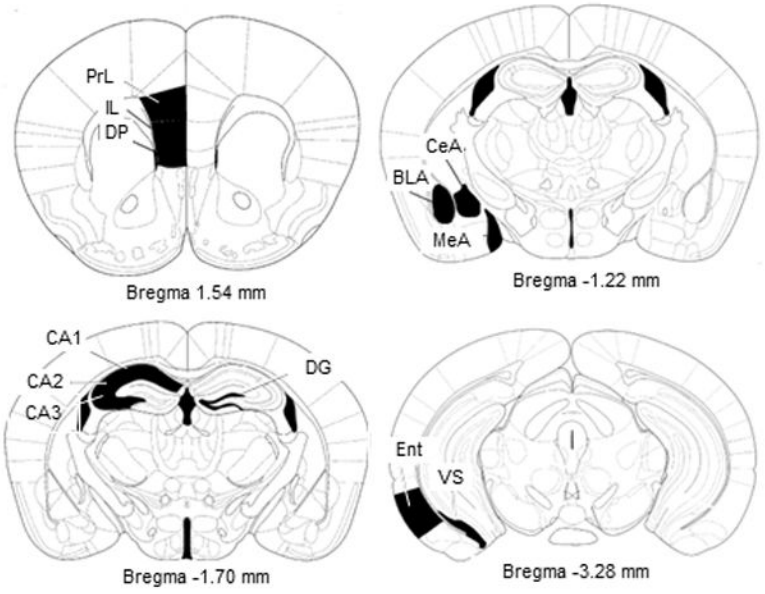

Figure 1.

Schematics of brain regions analyzed for DEK-positive immunolabeling. Abbreviations: prelimbic cortex (PrL), infralimbic cortex (IL), dorsal peduncular cortex (DP), medial amygdala (MeA), central amygdala (CeA), basolateral amygdala (BLA), hippocampal formation, dentate gyrus (DG) cornu ammonis (CA1, CA2, CA3), entorhinal cortex (Ent), and ventral subiculum (VS).

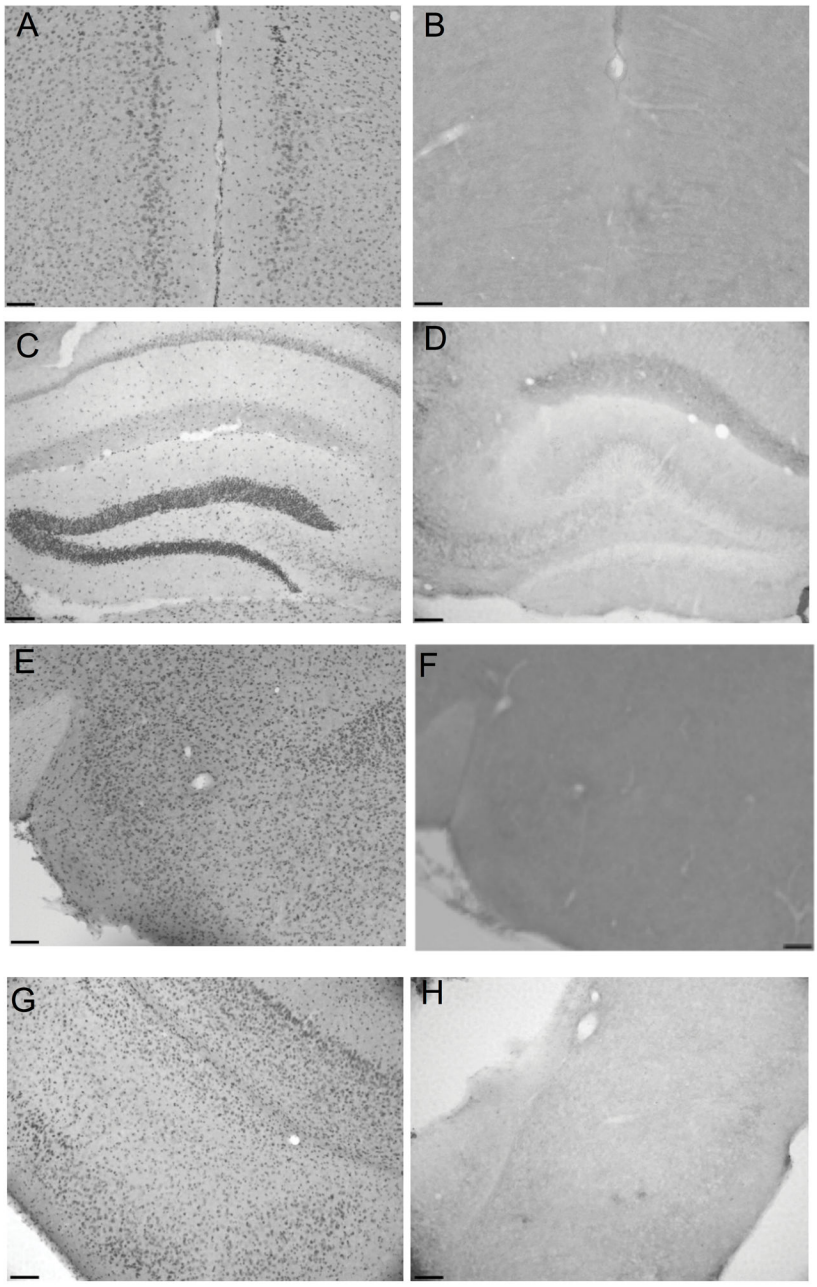

Figure 2.

DEK immunolabeling in adult wild-type **(A, C, E, G)** and Dek KO **(B, D, F, H)** mice in the medial prefrontal cortex **(A and B),** dorsal hippocampus **(C and D),** amygdala **(E and F)** and entorhinal cortex and ventral subiculum **(G and H)**. Wild-type (n=5) and DeK KO (n=6). Scale bars = 100 μm.

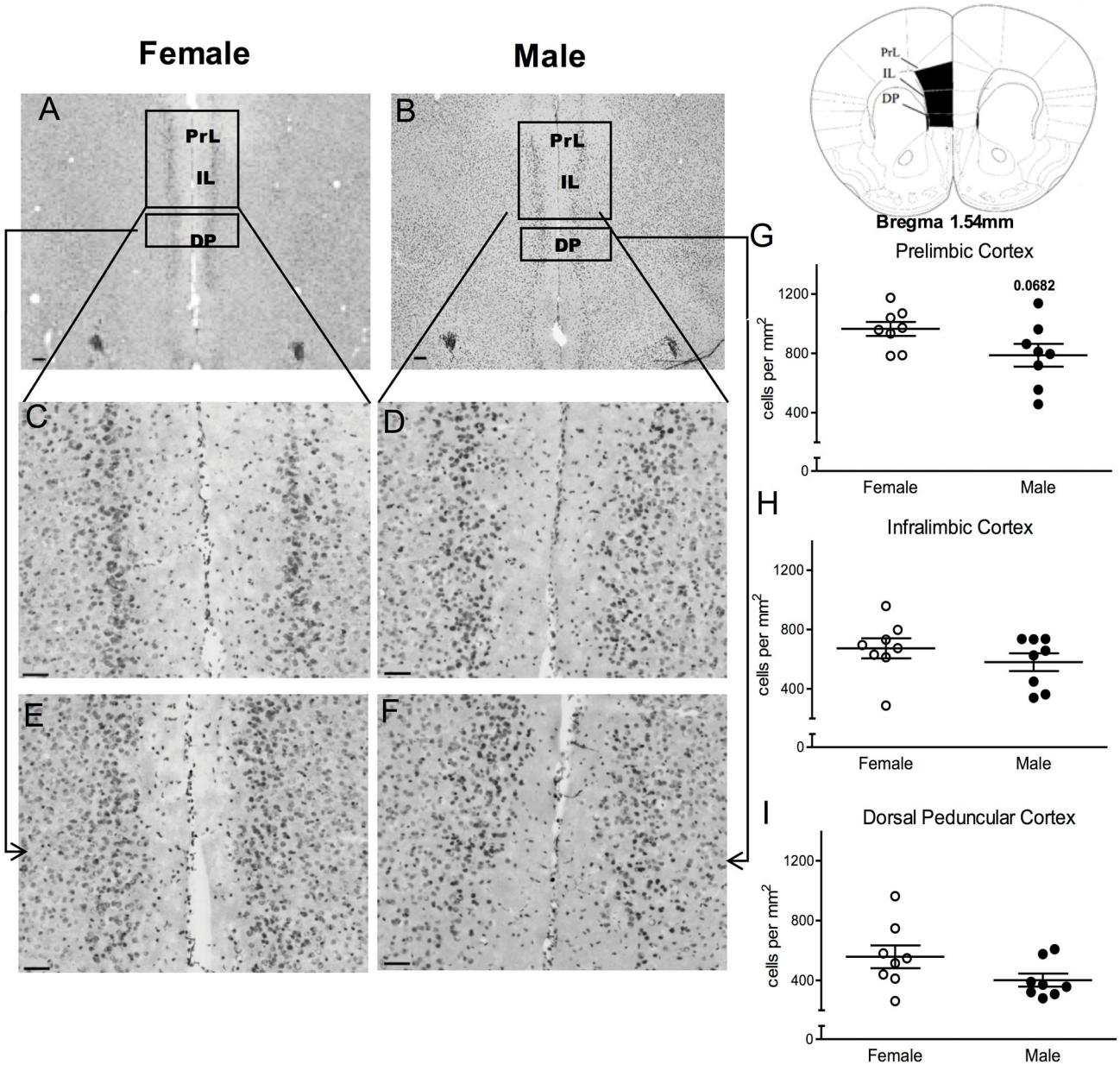

Figure 3.

Representative photomicrograph of DEK immunoreactivity in the prelimbic cortex (PrL), infralimbic cortex (IL), and dorsal peduncular nucleus in adult **(A)** female and **(B)** male c57BL/6 mice at 5x magnification. DEK immunoreactivity in the PrL/IL and DP in a female **(C and E)** and male mouse **(D and F)** at 10x magnification, respectively. There is no sex difference in DEK expression in any subdivision of the medial prefrontal cortex **(G–I)**. Data are expressed as individual data plots with the mean as a superimposed horizontal line with the standard error of the mean. Scale bars = 100 μm **(A and B)** and 50 μm **(C–F).** For all brain regions, females (n=8) and males (n=8).

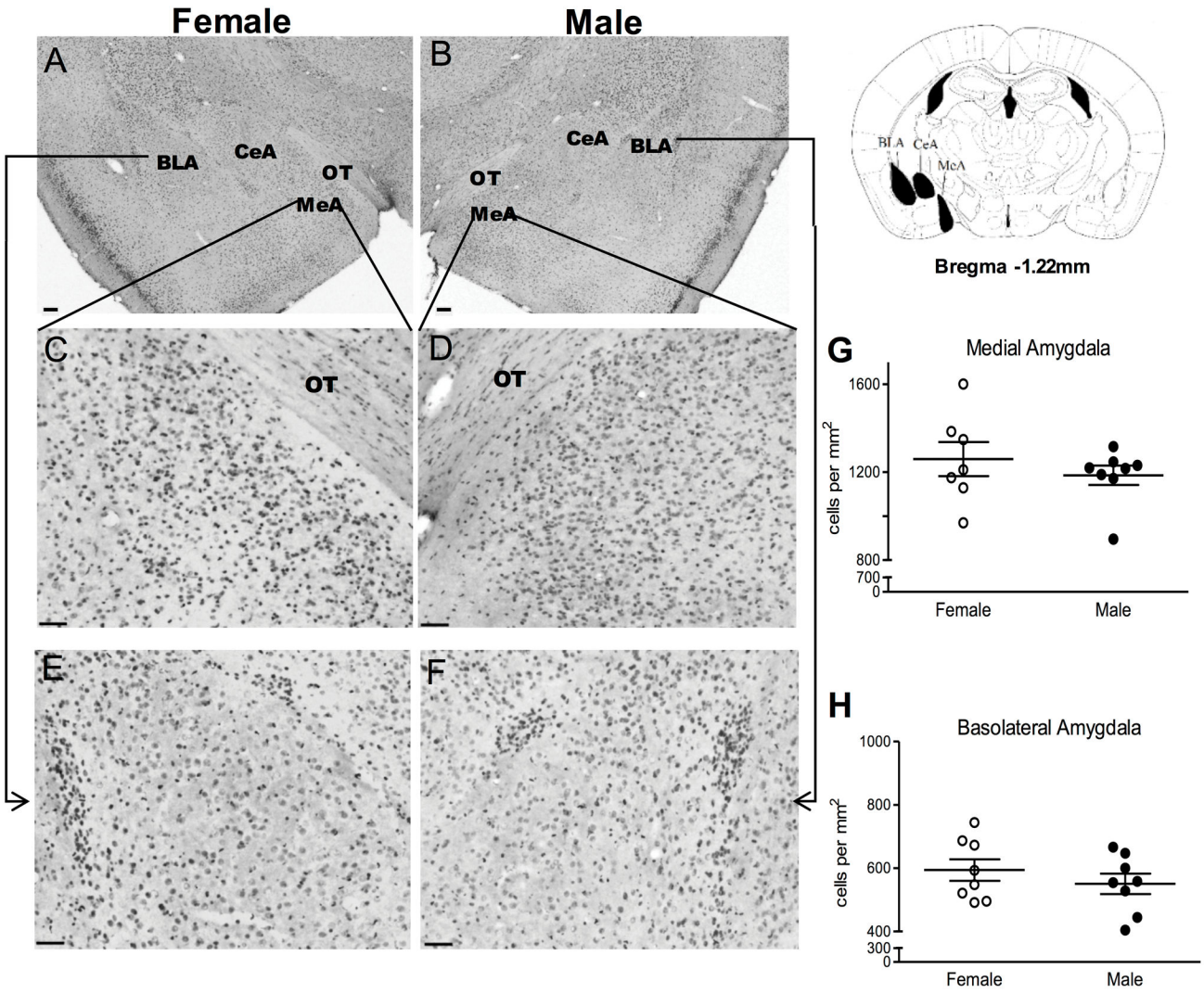

Figure 4.

Representative photomicrograph of DEK immunoreactivity for amygdalar subdivisions including the basolateral amygdala (BLA), central amygdala (CeA) and medial amygdala (MeA) in adult **(A)** female and male **(B)** c57BL/6 mice at 5x magnification. DEK immunoreactivity in the MeA and BLA in a female **(C and E)** and male **(D and F)** mouse at 10x magnification, respectively. There is no sex difference in DEK expression in the MeA **(G)** or in the BLA **(H)**. ot= optic tract. Data are expressed as individual data plots with the mean as a superimposed horizontal line with the standard error of the mean. Scale bars = 100 μm (**A and B)** and 50 μm **(C–F)**. Medial amygdala; males (n=7) and females (n=7) and for basolateral amygdala; females (n=8) and males (n=8).

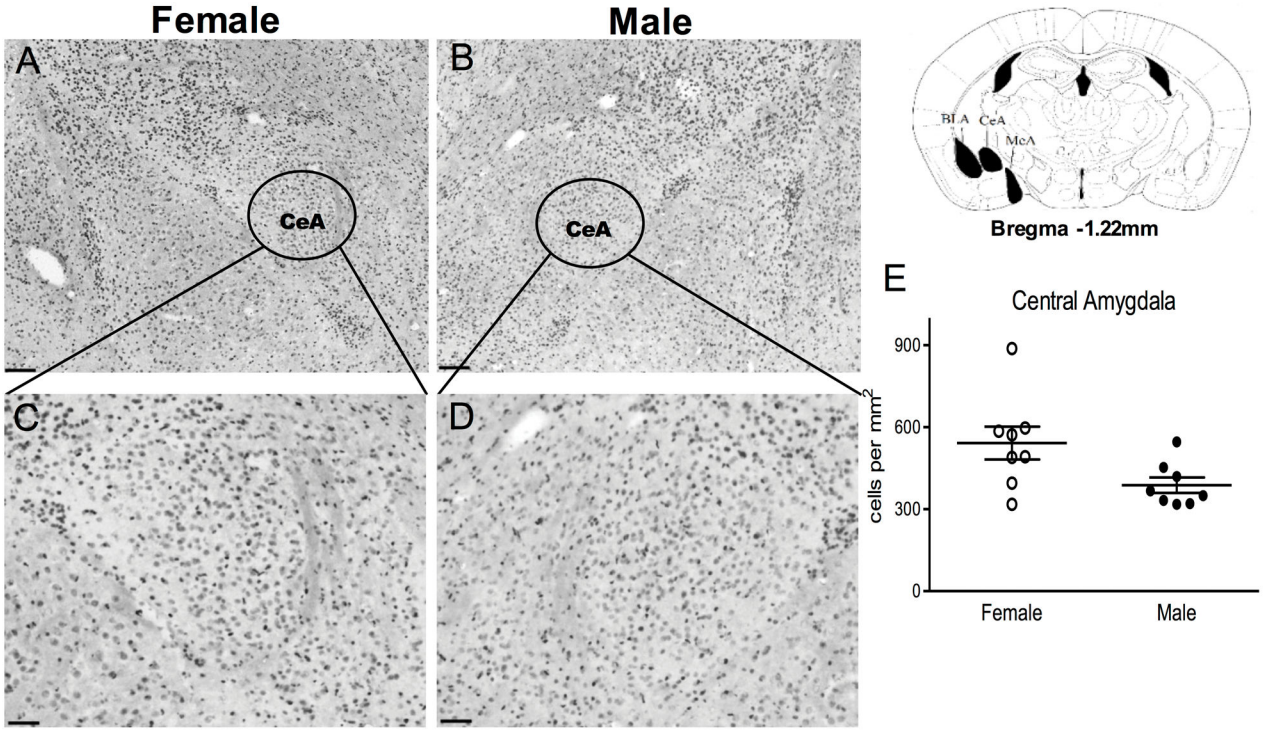

Figure 5.

DEK immunoreactivity in the CeA of an adult female **(A and C)** and male **(B and D)** c57BL/6 mouse. **(E)** There is no sex difference in DEK expression in the CeA. Data are expressed as individual data plots with the mean as a superimposed horizontal line with the standard error of the mean. Scale bars = 100 μm **(A and B)** and 50 μm (**C and D).** Females (n=8) and males (n=8).

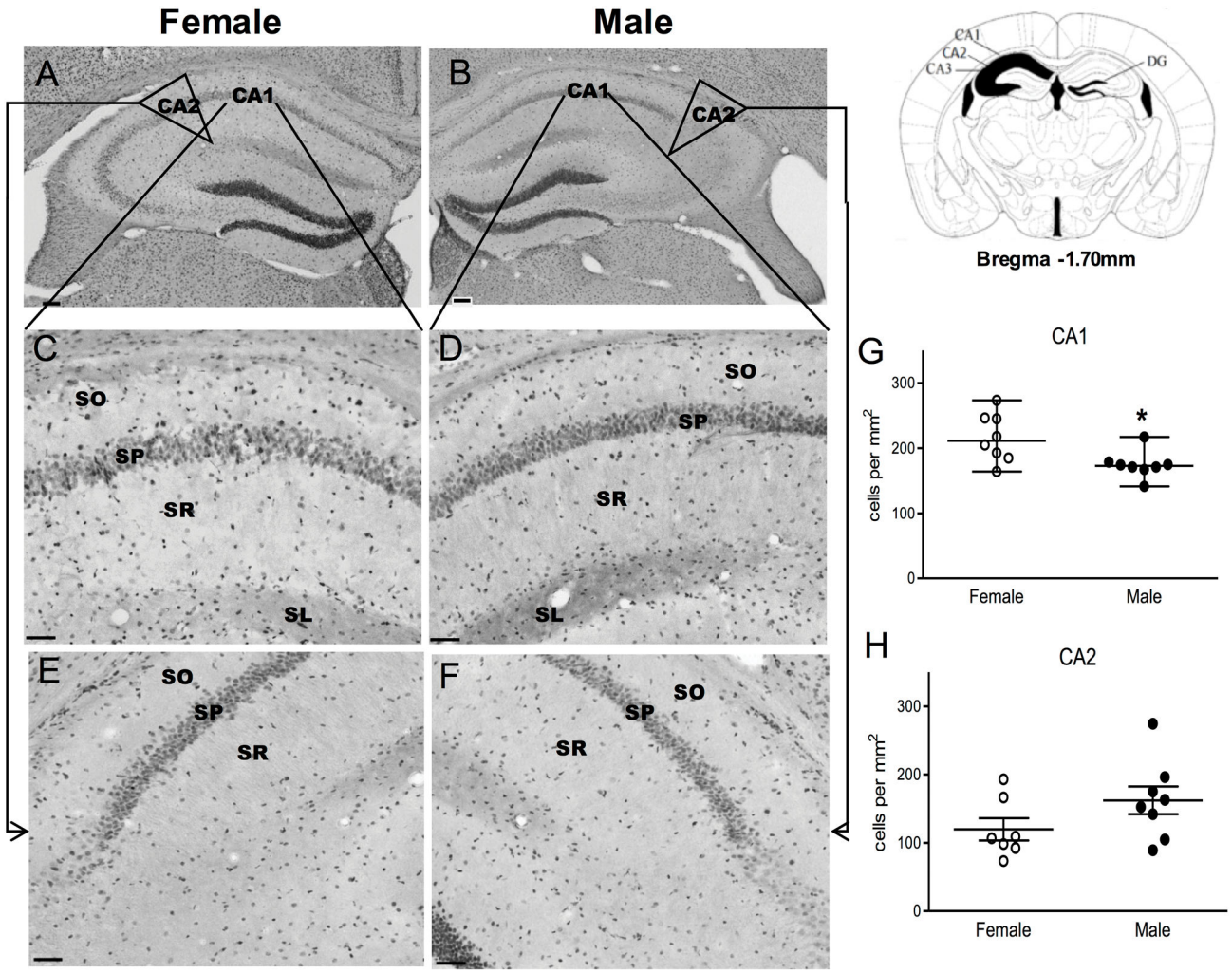

Figure 6.

Representative photomicrograph of DEK immunoreactivity in the cornu ammonis CA1, CA2, CA3, and dentate gyrus (DG) divisions of the dorsal hippocampus in adult female **(A)** and **(B)** male c57BL/6 mice at 5x magnification. DEK immunoreactivity in the CA1 and CA2 of a female **(C and E)** and male **(D and F)** mouse at 10x magnification, respectively. Females have significantly higher DEK expression in the CA1 relative to males **(G)**. There is no sex difference in DEK expression in CA2 **(H).** Stratum oriens (SO), stratum pyramidale (SP), stratum radiatum layer (SR), and stratum lacunosum moleculare (SL). Data for CA1 are expressed as individual data plots with the median as a superimposed horizontal line with the range; while the CA2 data are expressed as individual data plots with the mean as a superimposed horizontal line with the standard error of the mean. Scale bars = 100 μm **(A and B)** and 50 μm (**C and D)**, and * is $p < .05$. Females; CA1 (n=8) CA2 (n=7) and males (n=8) for CA1 and CA2.

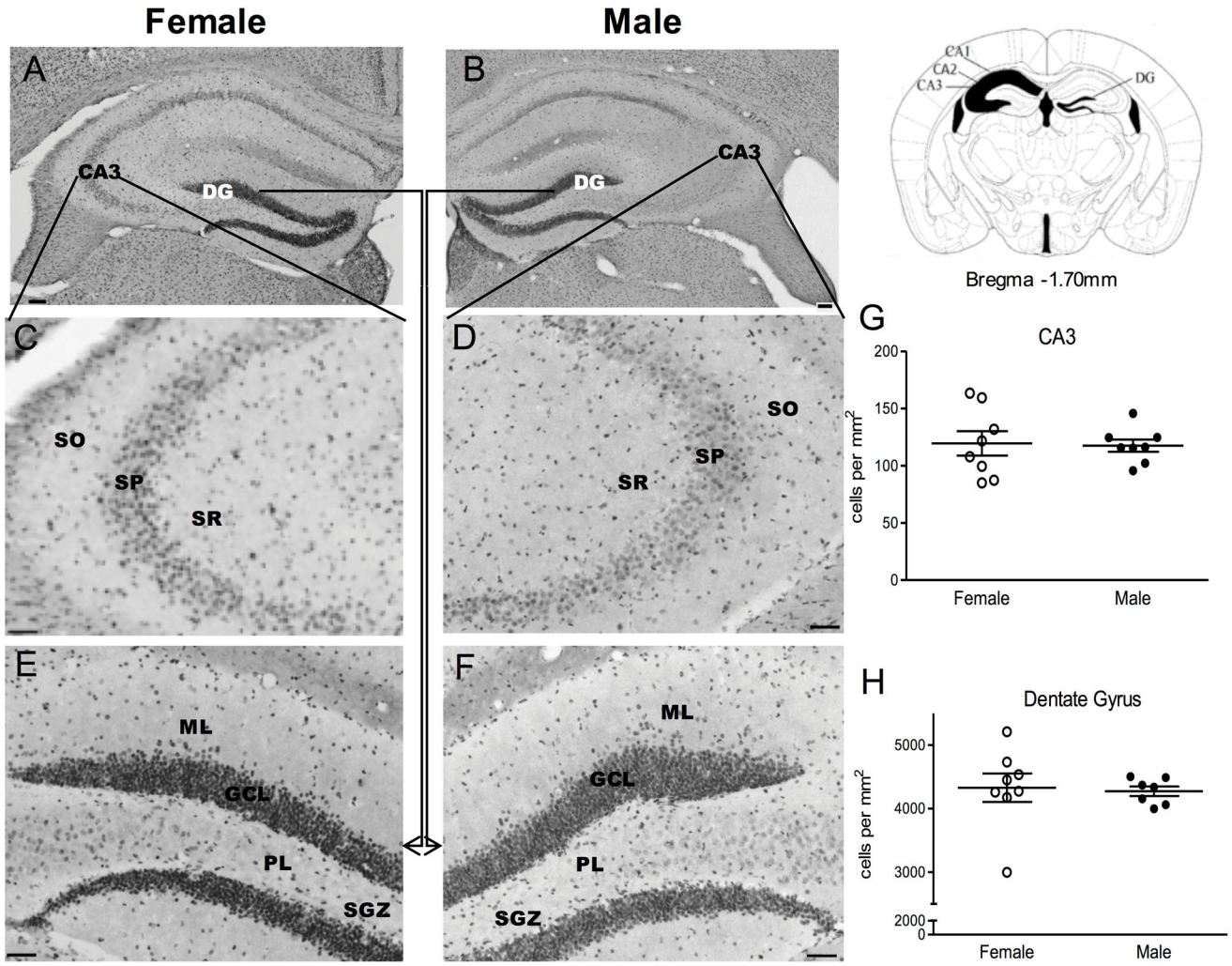

Figure 7.

Representative photomicrograph of DEK immunoreactivity in the cornu ammonis CA1, CA2,CA3, and dentate gyrus (DG) divisions of the dorsal hippocampus in adult female **(A)** and **(B)** male c57BL/6 mice at 5x magnification. DEK immunoreactivity in the CA3 and DG in a female **(C and D)** and male **(D and F)** mouse at 10 x magnification, respectively. There is no sex difference in DEK expression in CA3 **(G)** or DG **(H)**. Stratum oriens (SO), stratum pyramidale (SP), stratum radiatum layer (SR), stratum lacunosum moleculare (SL), molecular layer (ML) granule cell layer (GCL), polymorph (PL) and subgranular zones (SGZ). Data are expressed as individual data plots with the mean as a superimposed horizontal line with the standard error of the mean. Scale bars = 100 μm **(A and B)** and 50 μm (**C and D).** Females (n=8) and males (n=8).

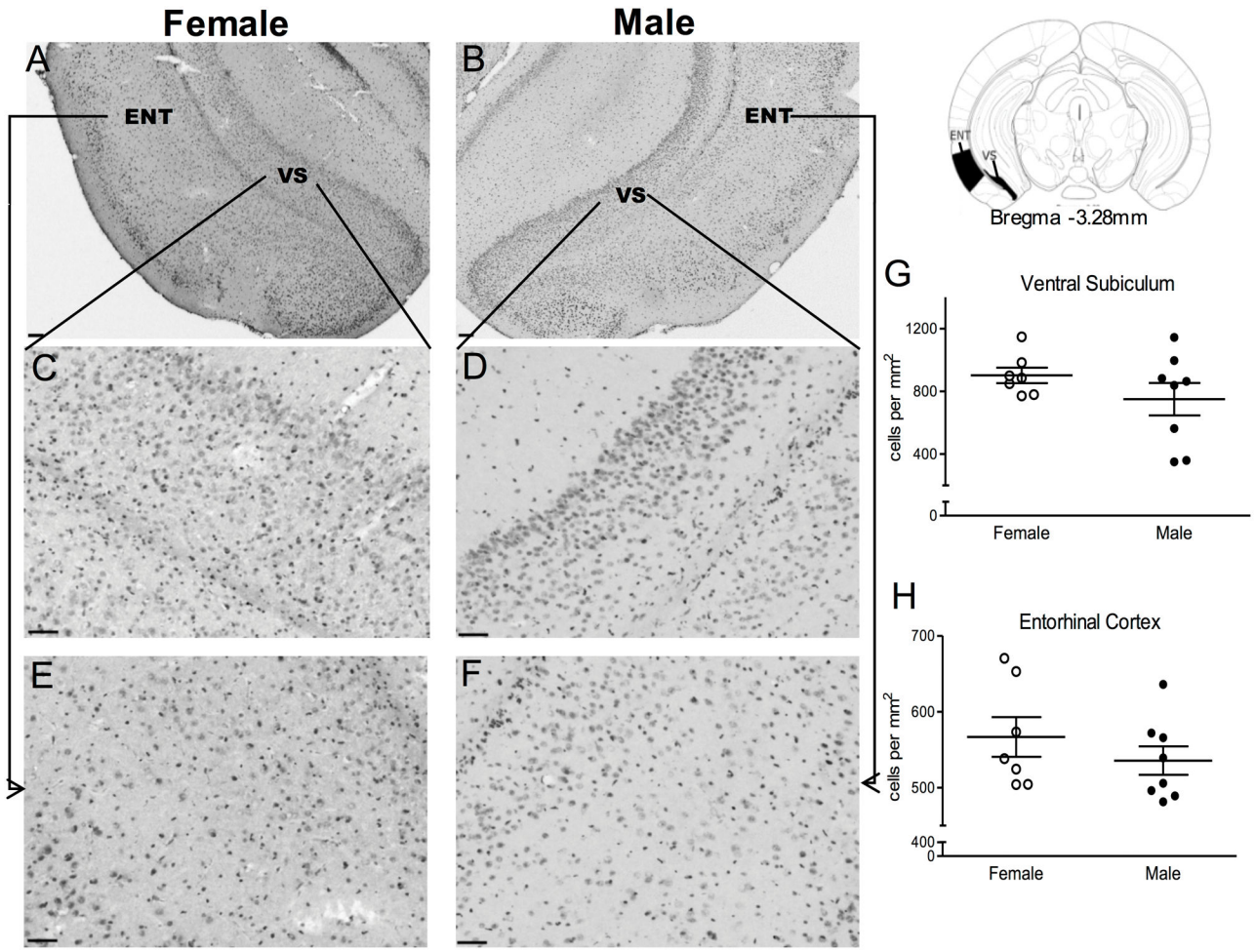

Figure 8.

Representative photomicrograph of DEK immunoreactivity in the ventral subiculum (VS) and entorhinal cortex (ENT) for adult female **(A)** and **(B)** male c57BL/6 mice at 5x magnification. DEK immunoreactivity in the VS and ENT in a female **(C and E)** and male **(D and F)** mouse, respectively. There is no sex difference in DEK expression in VS **(G)** or ENT **(H)**. Data are expressed as individual data plots with the mean as a superimposed horizontal line with the standard error of the mean. Scale bars = 100 μm for **(A and B)** and 50 μm **(C–F)**. Females (n=7) and males (n=8).

Table 1

Diseases associated with DEK loss of function

Disease	p value	Genes from dataset	Genes in Annotation
	3.006E-15	191	1587
	6.994E-13	186	1621
	2.103E-12	214	1969
Rheumatoid Arthritis	6.098E-11	114	1541
Arthritis	8.077E-11	53	496
Degenerative polyarthritis	2.151E-10	74	75
Colon Carcinoma	3.930E-10	147	1851
	5.550E-7	28	251
	6.055E-7	25	206
	7.558E-7	35	331
	1.328E-6	44	298
Autoimmune Diseases	5.045E-6	61	757
	8.771E-6	5	6
Inflammation	9.70E-06	17	110
	1.785E-5	56	456
	1.941E-5	73	937
	3.73E-05	60	772
	4.06E-05	5	10
	5.032E-4	5	11
	3.536E-4	3	3

Gene ontology analysis (partial list) of diseases associated with DEK loss of function in UMSCC1 HNSCC cell line. Diseases marked in blue (cancer-related) and black (inflammatory) are known DEK associated diseases. Cognitive-related diseases in red are for the first time associated with DEK loss of function. RNA-Seq previously published in (Adams et al 2015a).